

SUPPLEMENTARY INFORMATION

FOXO1 and FOXO3 transcription factors have unique functions in meniscus development and homeostasis during aging and osteoarthritis

Authors

Kwang Il Lee¹, Sungwook Choi^{1,2}, Tokio Matsuzaki¹, Oscar Alvarez-Garcia¹, Merissa Olmer¹, Shawn P. Grogan¹, Darryl D. D'Lima¹ and Martin K. Lotz¹

¹Department of Molecular Medicine, The Scripps Research Institute, La Jolla, CA, 92037

²Department of Orthopaedic Surgery, Jeju National University College of Medicine, 63243, Jeju, South Korea

Corresponding Author: Martin K. Lotz, Department of Molecular Medicine, Scripps Research, 10550 North Torrey Pines Road, La Jolla, CA 92037, Phone: (858) 784-8960; mlotz@scripps.edu

This PDF file includes:

SI Materials and Methods
Figures S1 to S11
Table S1
SI References

SI Materials and Methods

Human meniscus tissues from normal, aging and OA knees

Normal human knee joints were obtained from tissue banks (approved by Scripps Institutional Review Board). Knees were collected by resection of femur, tibia and fibula 15 cm above and below the joint line. The knees were received within 48h postmortem. Subjects with a history of knee trauma were excluded. Macroscopic and microscopic grading of the articular cartilage in all knee compartments was performed with a modified Outerbridge system as described (1-3). Menisci were also obtained from OA joints at the time of knee arthroplasty. We reported previously on macroscopic and histopathologic analysis of human knee menisci in aging and OA (4). In the previous study, 6 cases in 3 groups (Young; old; Osteoarthritis) were randomly selected for analysis. In this study, young (Avg. age 25 ± 1 , $n=6$), aging (Avg. age 56 ± 1 , $n=6$), and OA (Avg. age 72 ± 6 , $n=6$) were analyzed with the same methods of the previous study (4).

Mouse aging model

All animal studies were performed with approval by the Scripps Institutional Animal Care and Use Committee. Pathogen-free C57BL/6J mice were purchased from the Scripps Research Institute breeding facility. The mice were sacrificed at various ages and knee joints were collected for analysis. Both male and female mice were included in this study. A total of 18 mice at three different ages were assessed: 6 ($n = 6$), 12 ($n = 6$), and 24 ($n = 6$) month old mice. We performed histological and immunohistochemical analyses in the 3 age groups and quantified changes in different zones of the anterior horn and posterior horn of the menisci as illustrated in Fig. S2.

Mice with conditional postnatal FoxO deletion

Col2a1-Cre/+ transgenic mice (5, 6) and Aggrecan (Acan)-CreERT2 knockin mice (7) on a C57BL6/J background were obtained from The Jackson Laboratory (JAX#003554, Bar Harbor, ME, USA). FoxO1^{lox/lox}, FoxO3^{lox/lox} and FoxO4^{lox/lox} were obtained from Dr. R. DePinho (The University of Texas MD Anderson Cancer Center, Houston, TX) (8). With Col2Cre, we generated mice with deletion of individual FoxO 1, 3 or 4 and mice with deletion of FoxO1, 3 and 4 (FoxO triple KO, FoxO TKO) mice. In the AcanCreERT2 model, we bred AcanCreERT2/+ knockin mice with FoxO1^{lox/lox}; FoxO3^{lox/lox}; FoxO4^{lox/lox} triple transgenic mice to obtain AcanCreERT2-TKO mice. Tamoxifen (Sigma-Aldrich, St. Louis, MO, USA) was intraperitoneally injected at a dose of 1.5mg/10g body weight on 5 consecutive days in 4-month-old mice. Genotyping was performed by PCR using tail DNA. Littermates homozygous for the floxed FoxO not expressing Cre recombinase were used as controls of Col2Cre-FoxO KO mice, and AcanCreERT2/- littermates that were also injected with tamoxifen as controls of AcanCreERT2-TKO mice. Knee joints were collected from 1-, 2-, 4-, 6-, 12-month-old control, Col2Cre-TKO and Col2Cre-FoxO1/3/4 single KO mice. In addition, knee joints were collected from control and AcanCreERT2-TKO mice 5 months after tamoxifen injection.

Surgical and treadmill running induced OA models

Surgical OA model was created by destabilizing the medial meniscus (DMM) (9) in 6-months-old mice. In the treadmill-induced OA model, 6-months-old mice were placed on a treadmill (Columbus Instruments Exer 3/6 Treadmill, Columbus, OH) at 10 degrees incline for 45 minutes at a speed of 15 m/min including 2 minutes warming up (10). Mice were euthanized 8 weeks after DMM surgery and 6 weeks after treadmill exercise, and six knee joints at each group were collected.

Histological analyses of mouse joints

The entire knee joints were fixed in 10% zinc buffered formalin for 2 days, decalcified in TBD-2 (Decalcifier, Thermo Fisher Scientific) for 24 h. Sections of the mouse knee joints were stained with Safranin-O–fast green for further analysis.

Immunohistochemistry

Knee joint sections were deparaffinized, washed and blocked with 10% goat serum for 1 h at room temperature. Primary antibodies against FoxO1A (1:250, Abcam, Cambridge, MA), FoxO3A (1:500, Abcam), and FoxO4 (1:250, Abcam) were applied in 0.1% Tween 20 and incubated overnight at 4°C, followed by secondary antibody using ImmPRESS reagents (Vector Laboratories, Burlingame, CA, USA). All antibodies were of rabbit origin and rabbit IgG staining was used as negative control (Fig. S10). The signal was developed with diaminobenzidine (DAB, Sigma-Aldrich) and counterstained with methyl green or hematoxylin.

Quantification of immunohistochemistry

For quantification of changes in the mouse or human tissues, menisci were divided into vascular, avascular, and superficial zones (Fig. S2). The number of positive cells per field was counted under a microscope at the 40× magnification for each of the 3 zones from each meniscus section. The percent positive cells per field was determined as the ratio of the total number of positive cells to the total cell number of meniscus in the respective zone.

RNA and protein isolation from menisci

Entire menisci were collected from both sides of the knee joints of 2-month-old and 5-month-old mice (n=6 each). For human menisci, vascular and avascular zones were separated from OA patients (70±4 years; 4 females, 2 males) and young normal cadavers (19±1 years; 6 males) for RNA extraction. Total RNA was extracted from mouse meniscus tissues or cultured meniscus cells using TRIzol (Invitrogen, Carlsbad, CA), followed by Zymo Direct-zol RNA MiniPrep kits

(Zymo Research, Irvine, CA). Human meniscus tissue was resuspended in RNA-later (Qiagen, Valencia, CA) immediately after harvest and stored at -20°C until RNA extraction. For RNA isolation, meniscus tissues were homogenized in Qiazol Lysis Reagent (Qiagen, Valencia, CA) at a concentration of 25mg tissue sample per 700ul Qiazol. RNA was extracted from meniscus using the fibrous tissue RNA extraction kit (Qiagen). RNA was isolated using RNAqueous kit (Ambion, Carlsbad, CA) and then, on-column DNase treatment was performed using the DNase I (Qiagen, Valencia, CA) and the RNeasy MinElute Cleanup kit (Qiagen, Valencia, CA). Protein was extracted from human vascular and avascular meniscus from same patients and cadavers used for RNA extraction. Protein extracts were prepared with RIPA Lysis and Extraction Buffer (Fisher, Waltham, MA). Protein concentrations were measured by BCA protein assay kit (Bio-Rad, Hercules, CA).

PCR

Quantitative-PCR analysis was conducted on a LightCycler 480 Real-Time PCR System (Roche Diagnostics, Indianapolis, IN) with up to 45 cycles using TaqMan Gene Expression Assay probes (Life Technologies, online Table S1). The levels of mRNA were calculated as relative quantities in comparison to Gapdh (Fig. S11).

Western blotting

Western blotting was performed with the Licor Odyssey immunofluorescence detection system (LI-COR Biosciences, Lincoln, NE). Equal amounts of protein were separated on 4-20% SDS PAGE gels and transferred to nitrocellulose membranes. As primary antibodies, FoxO1 and FoxO3 antibodies were used. As secondary antibodies, goat anti-mouse-IRDye 680 (1:10,000) and goat anti-rabbit-IRDye 800 (1:5,000) (LI-COR Biosciences) were used.

Statistical analyses

Results were analyzed using Prism version 5.2 (GraphPad Software, Inc., La Jolla, CA). A Mann-Whitney t test was used to establish statistical significance between two groups in the qRT-PCR results. Two-way ANOVA test was used for multiple comparisons between groups in the histopathology analyses. Variance was used to compare multiple groups, with subsequent pairwise (group) comparisons assessed at an experiment-wise error level of 0.05. P values less than 0.05 were considered statistically significant.

Table S1

PCR probe information

Mouse gene	Probe	Human gene	Probe
<i>Gapdh</i>	Mm99999915_g1	<i>Gapdh</i>	Hs02758991_g1
<i>FoxO1</i>	Mm00490671_m1	<i>FoxO1</i>	Hs00231106_m1
<i>FoxO3</i>	Mm00490673_m1	<i>FoxO3</i>	Hs00818121_m1
<i>FoxO4</i>	Mm00840140_g1	<i>FoxO4</i>	Hs00172973_m1
<i>Col1a1</i>	Mm00801666_g1	<i>Col1a1</i>	Hs00164004_m1
<i>Col2a1</i>	Mm01309565_m1	<i>Col2a1</i>	Hs00156568_m1
<i>Acan</i>	Mm00545794_m1	<i>Acan</i>	Hs00153936_m1
<i>Comp</i>	Mm00489490_m1	<i>Comp</i>	Hs00164359_m1
<i>Prg4</i>	Mm00502413_m1	<i>Prg4</i>	Hs00981633_m1
<i>Mkx</i>	Mm00617017_m1	<i>Mkx</i>	Hs00543190_m1
<i>Smad2</i>	Mm00487530_m1	<i>Smad2</i>	Hs00998187_m1
<i>Sox5</i>	Mm01264584_m1	<i>Sox5</i>	Hs00374709_m1
<i>Sox9</i>	Mm00448840_m1	<i>Sox9</i>	Hs01001343_g1
<i>Runx2</i>	Mm00501584_m1	<i>Runx2</i>	Hs00231692_m1
<i>Col10a1</i>	Mm00487041_m1	<i>Col10a1</i>	Hs00166657_m1
<i>Mmp13</i>	Mm01168713_m1	<i>Mmp13</i>	Hs00233992_m1
<i>Sesn1</i>	Mm01185732_m1	<i>Sesn1</i>	Hs00902782_m1
<i>Sesn3</i>	Mm01171504_m1	<i>Sesn3</i>	Hs00914870_m1
<i>Gpx3</i>	Mm00492427_m1	<i>Gpx3</i>	Hs01078668_m1
<i>Map1lc3b</i>	Mm00782868_sH	<i>Map1lc3b</i>	Hs00797944_s1
<i>Becn1</i>	Mm01265461_m1	<i>Becn1</i>	Hs01007018_m1
<i>Gabarapl1</i>	Mm00457880_m1	<i>Gabarapl1</i>	Hs00740588)mH
<i>Bnip3</i>	Mm01275600_g1	<i>Bnip3</i>	Hs00969291_m1
<i>Prkaa2</i>	Mm01264789_m1	<i>Prkaa2</i>	Hs00178903_m1
<i>Catalase</i>	Mm00437992_m1	<i>Catalase</i>	Hs00156308_m1
<i>Sod2</i>	Mm01313000_m1	<i>Sod2</i>	Hs00167309_m1
<i>Txnip</i>	Mm01265659_g1	<i>Txnip</i>	Hs01006897_g1
<i>Adamts4</i>	Mm00556068_m1	<i>Adamts4</i>	Hs00192708_m1
<i>Adamts5</i>	Mm00478620_m1	<i>Adamts5</i>	Hs01095518_m1
<i>Il-6</i>	Mm00446190_m1	<i>Il-6</i>	Hs00174131_m1
<i>Ptgs2</i>	Mm00478374_m1	<i>Ptgs2</i>	Hs00153133_m1

Fig. S1

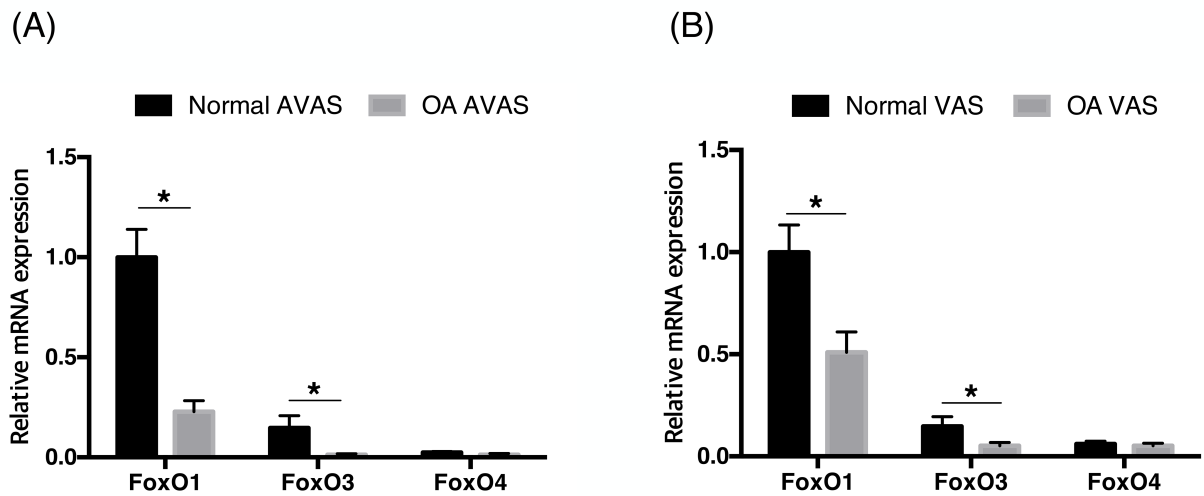


Fig. S1. FoxO mRNA expression in human meniscus. FoxO mRNA expression was analyzed by qRT-PCR in human normal and degenerated meniscus: (A) FoxO1, 3, and 4 mRNA expression in vascular meniscus; (B) FoxO1, 3, and 4 mRNA expression in avascular meniscus (n=6 per each group, *p<0.05).

Fig. S2

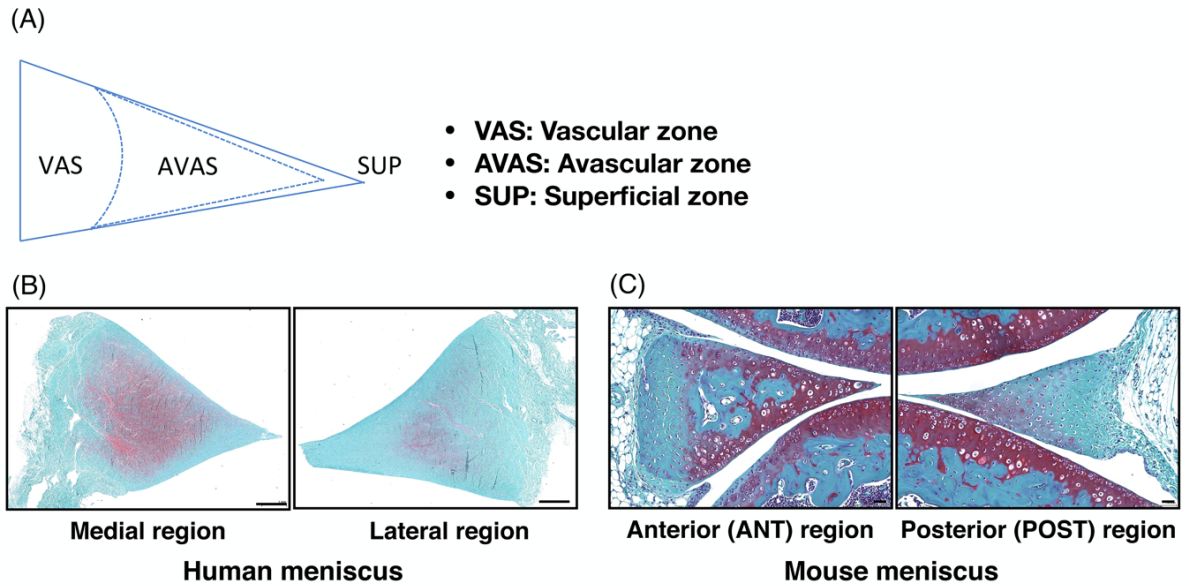


Fig. S2. Meniscus specific zones and regions for analysis. (A) Meniscus nomenclature (VAS: vascular; AVAS: avascular; SUP: superficial zone); (B) Human meniscus (medial and lateral regions, Scale bar: 1mm); (C) Mouse meniscus (anterior and posterior regions, Scale bar: 100um).

Fig. S3

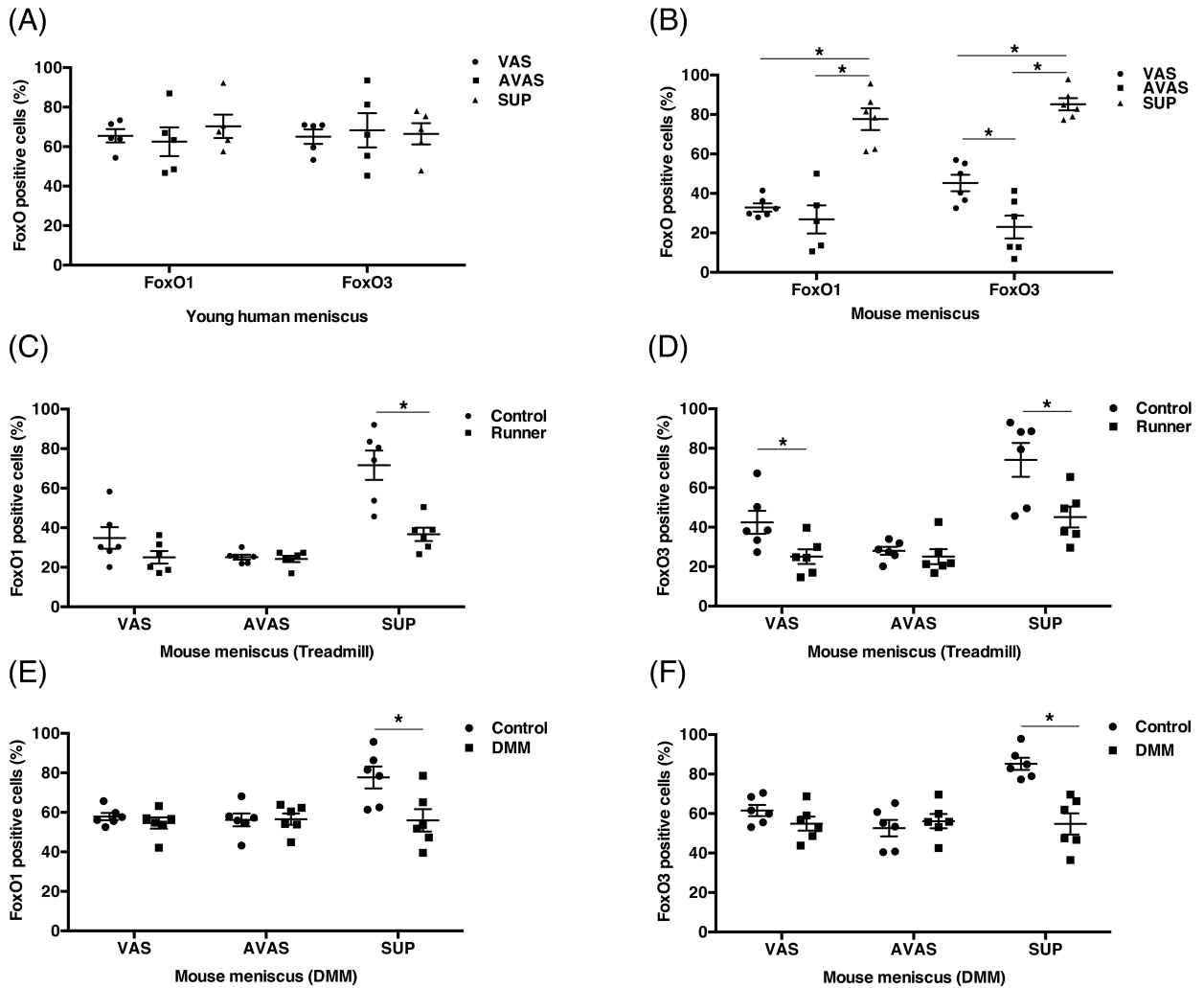


Fig. S3. FoxO expression in human and mouse meniscus. (A) FoxO1 and FoxO3 expression in different human (25±1years) meniscus regions; (B) FoxO1 and FoxO3 expression at different mouse (6 months old) meniscus regions.

Comparison of FoxO expression in different mouse (6 months old) meniscus regions between control and 6-week treadmill running model; (C) FoxO1 and (D) FoxO3

Comparison of FoxO expression in different mouse (6 months old) meniscus regions between control and 8-week post DMM surgery model; (E) FoxO1 and (F) FoxO3 (n=6 per group, *p<0.05).

Fig. S4

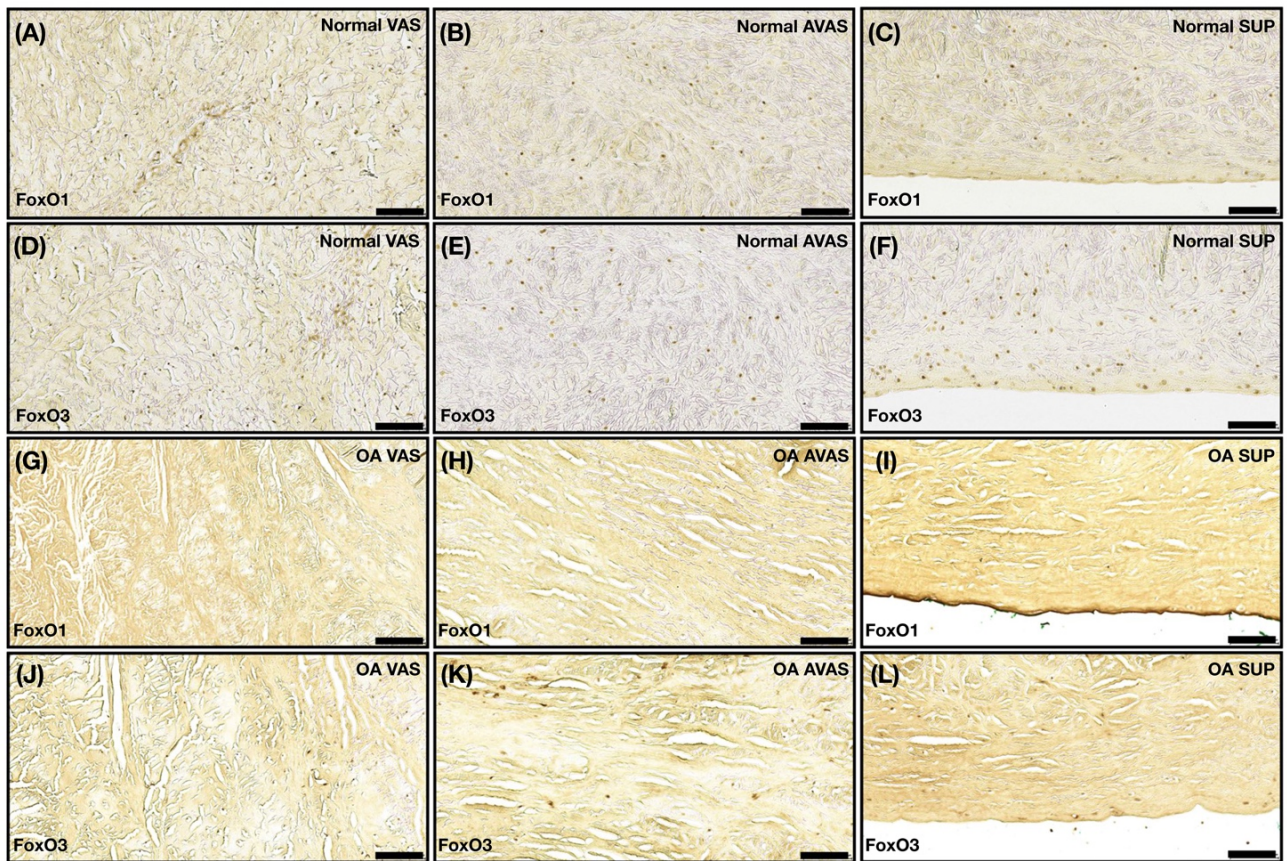


Fig. S4. FoxO expression in different meniscus zones. Immunohistochemistry of FoxO1 and FoxO3 in human meniscus vascular, avascular, and superficial zones. FoxO1 expression in normal meniscus: (A) vascular; (B) avascular; (C): superficial zone. FoxO3 expression in normal meniscus: (D) vascular; (E) avascular; (F): superficial zone. FoxO1 expression in OA meniscus: (G) vascular; (H) avascular; (I) superficial zone. FoxO3 expression in OA meniscus: (J) vascular; (K) avascular; (L) superficial zone. (Scale bar: 100um).

Fig. S5

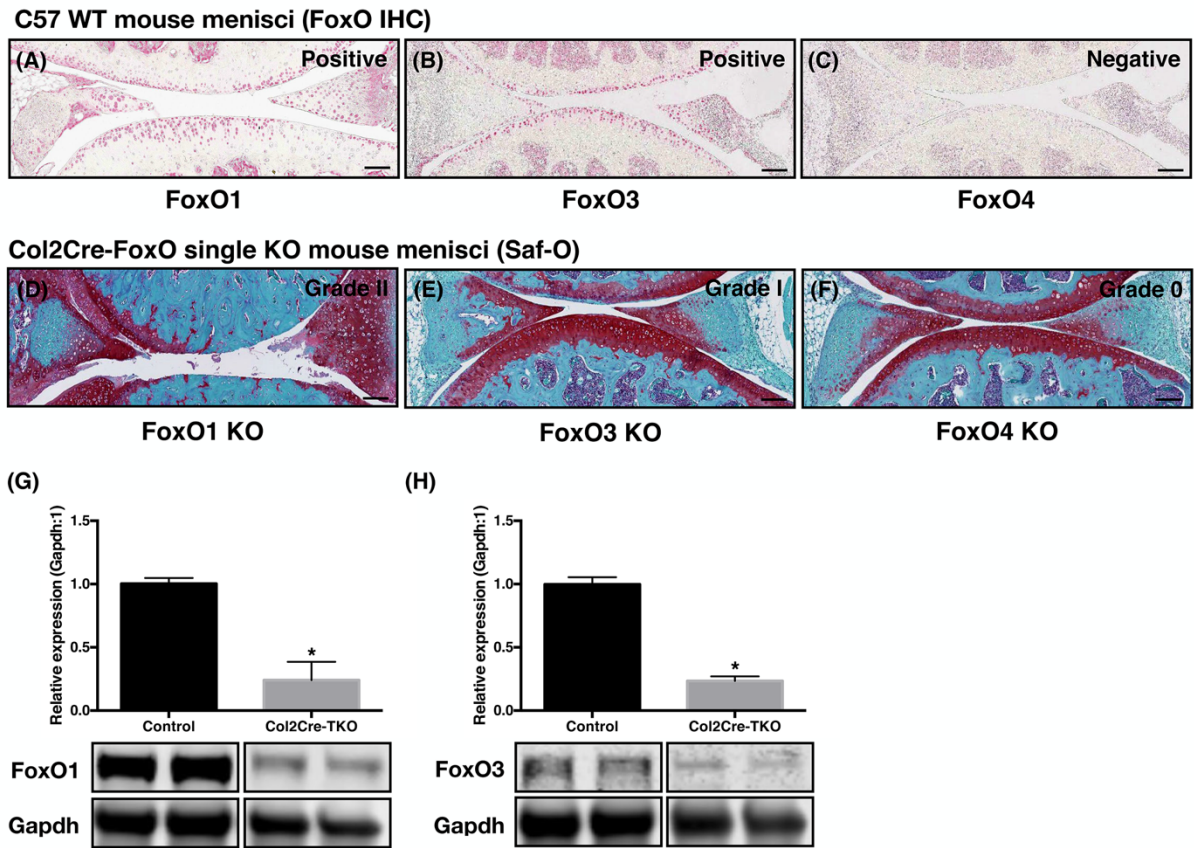


Fig. S5. FoxO expression in mouse meniscus. FoxO immunohistochemistry of WT mouse menisci (Age: 4M): (A) FoxO1; (B) FoxO3; (C) FoxO4 Safranin-O staining of Col2Cre-FoxO KO mouse menisci (Age: 4M): (D) FoxO1 KO mouse menisci; (E) FoxO3 KO mouse menisci; (F) FoxO3 KO mouse menisci (Scale bar: 100um)

Western blotting of proteins from Col2Cre-TKO mouse meniscus; (G) FoxO1 and (H) FoxO3 expression (Age: 4M, * $p < 0.05$).

Fig. S6

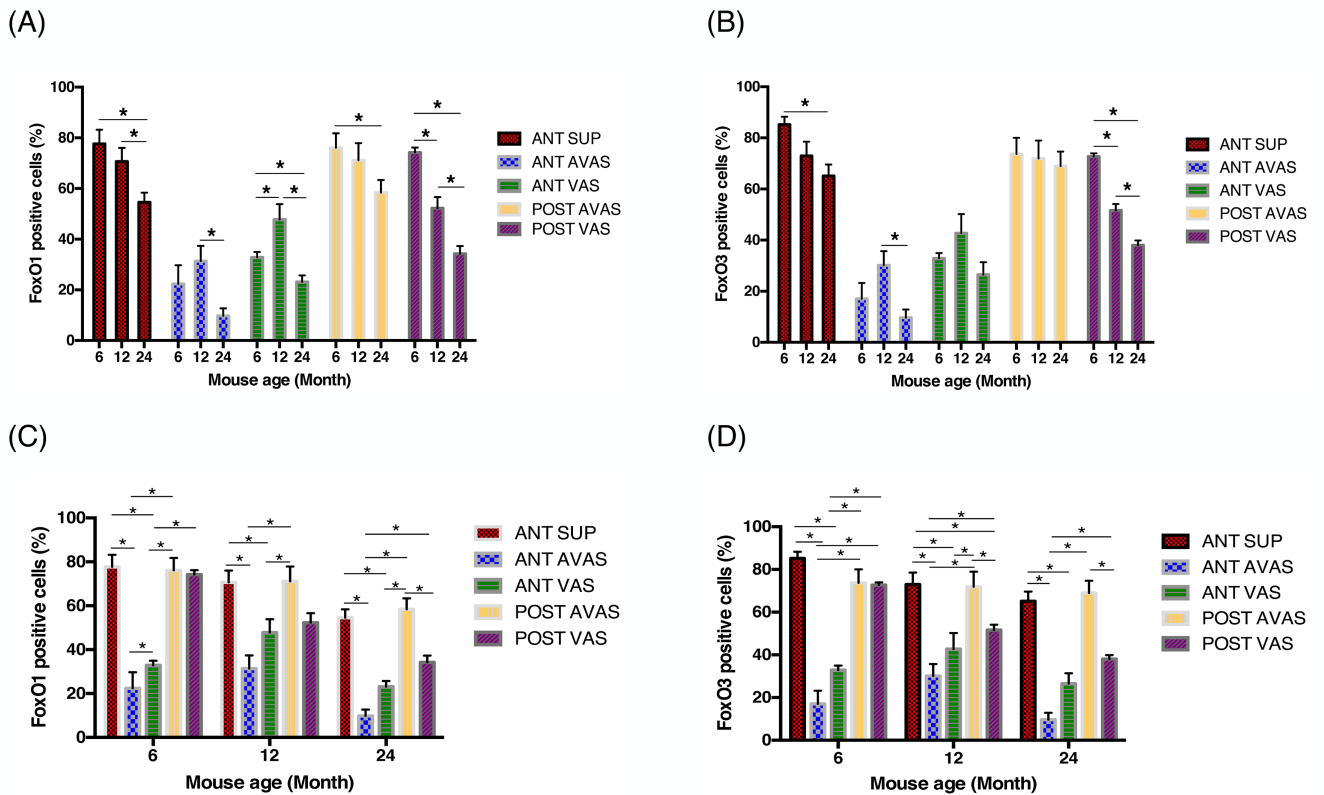


Fig. S6. FoxO expression in mouse meniscus regions in aging. FoxO1 and 3 changes in the normal mouse menisci: (A) FoxO1; (B) FoxO3 expression in aging was analyzed in specific meniscus regions (ANT SUP: anterior superficial region; ANT AVAS: anterior avascular region; ANT VAS: anterior vascular region; POST AVAS: posterior avascular region; POST VAS: posterior vascular region); (C) FoxO1; (D) FoxO3 expression in different meniscus region at each age (6, 12, 24-month old) (n=6 per each group, *p<0.05).

Fig. S7

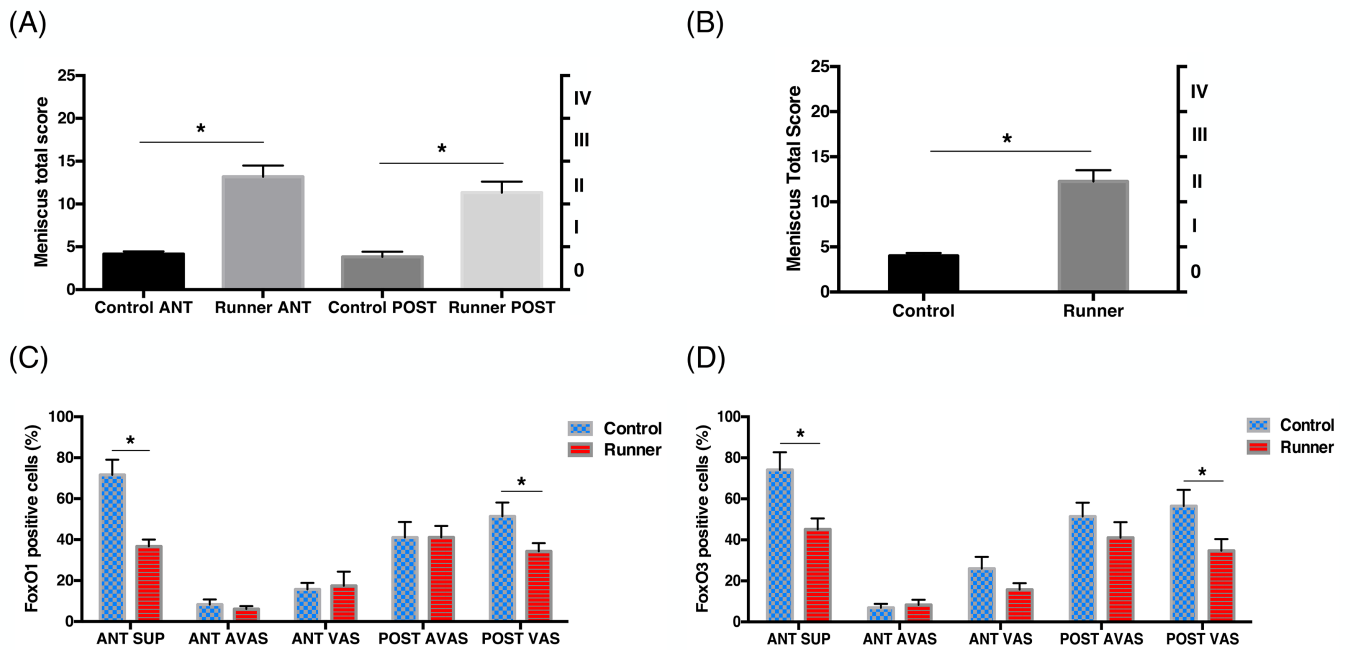


Fig. S7. FoxO expression in mice following treadmill running. FoxO1 and FoxO3 changes in the treadmill model after 6-week treadmill running: (A) FoxO1; (B) FoxO3 expression in different meniscus region; (C) Meniscus histological grading in anterior and posterior meniscus regions (n=6 per each group, *p<0.05).

Fig. S8

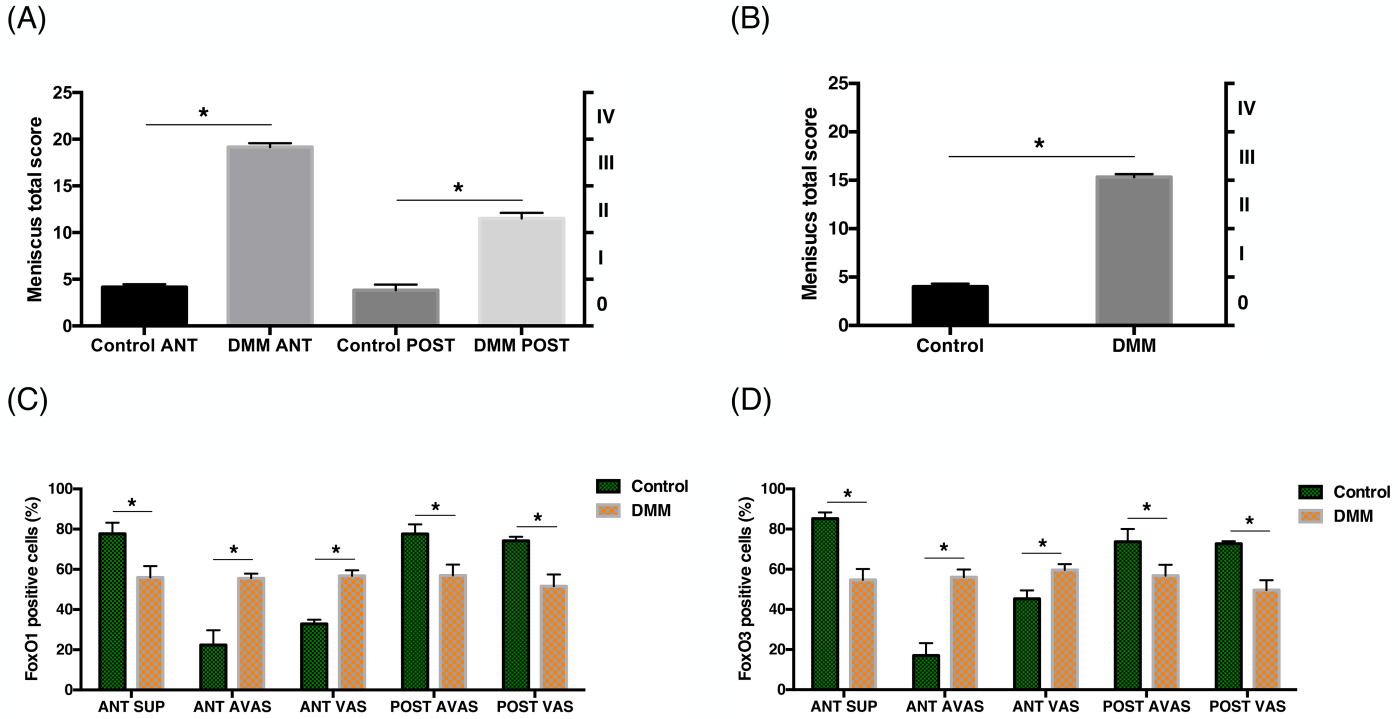


Fig. S8. FoxO expression in DMM surgical model. FoxO1 and FoxO3 changes in the DMM surgical model (8 weeks after surgery): (A) Meniscus histological grading in anterior and posterior meniscus regions; (B) Meniscus histological grading in control and DMM surgical model; (C) FoxO1; (D) FoxO3 expression in different meniscus region (n=6 per each group, *p<0.05).

Fig. S9

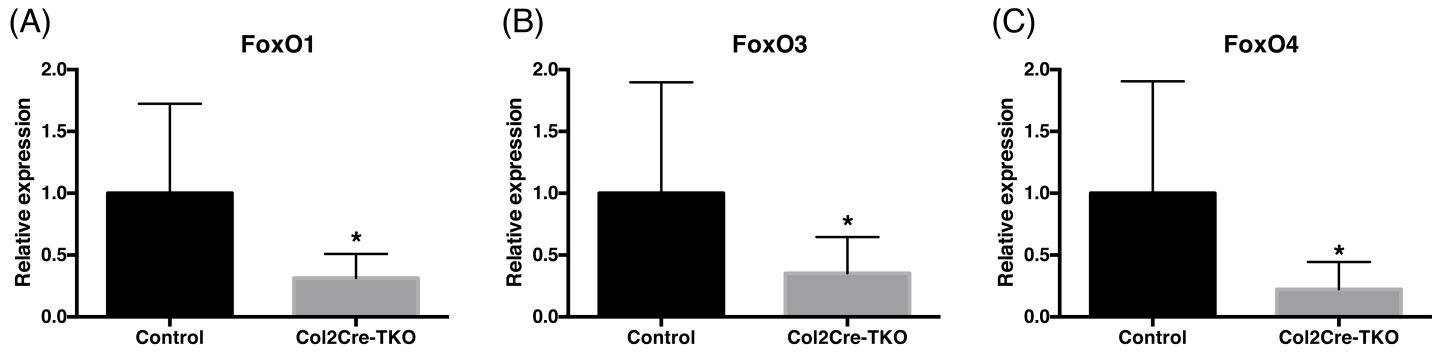


Fig. S9. FoxO gene expression in knock-out mice. Gene expression in Col2-Cre-FoxO TKO mouse menisci (6 months): (A) FoxO1; (B) FoxO3; (C) FoxO4.

Fig S10

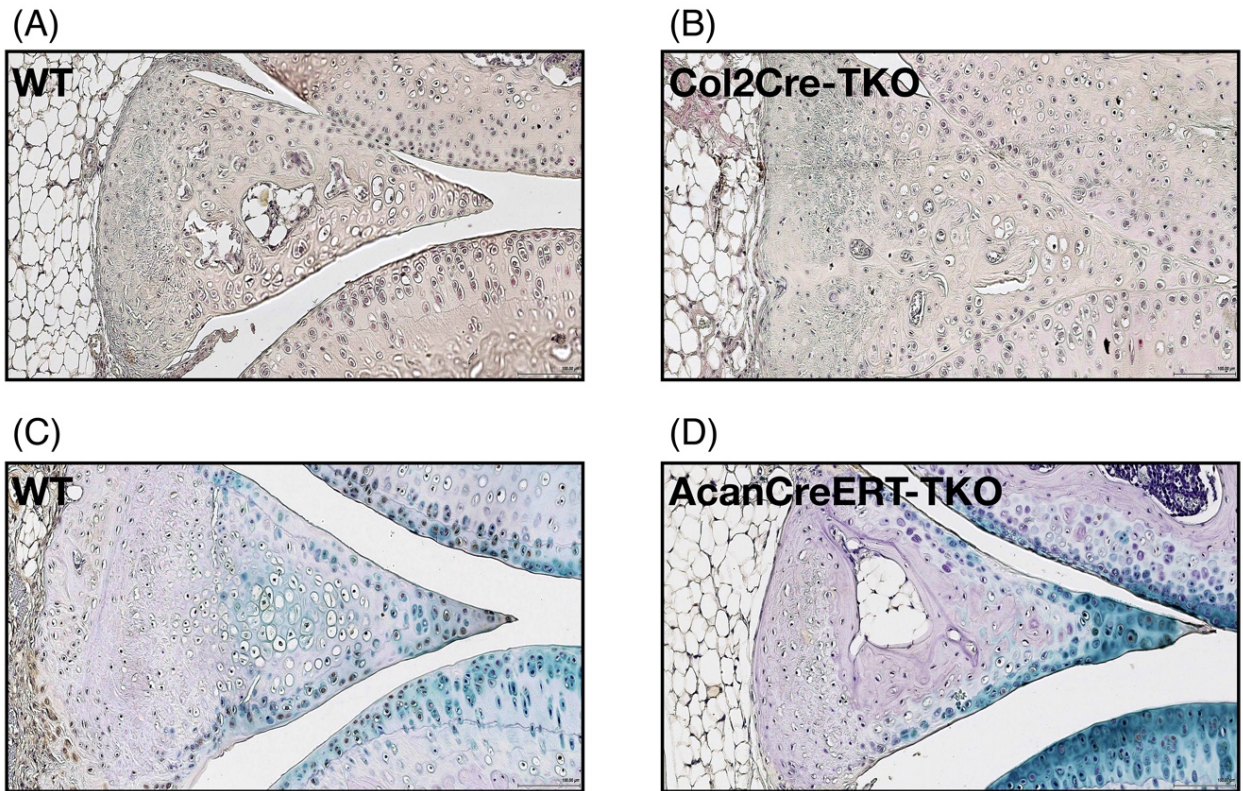


Fig. S10. Control antibodies in immunohistochemistry. Images show staining with Rabbit IgG. (A) Wild type and (B) Triple knockout type of Col2Cre-TKO; (C) Wild type and (D) Triple knockout type of AcanCre-TKO at 6 months old.

Fig. S11

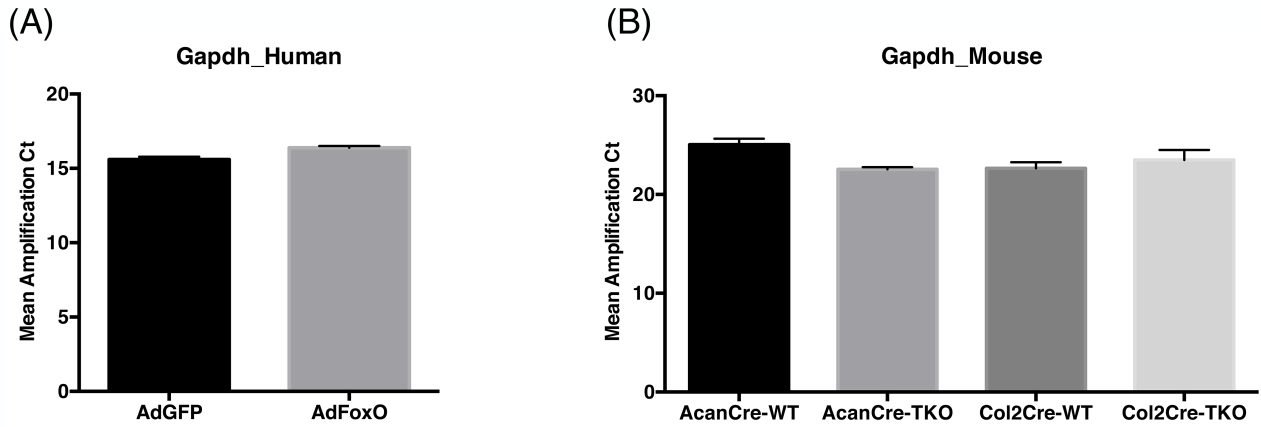


Fig. S11. Housekeeping gene expression in human and mouse menisci. (A) Human avascular meniscus cells transduced with AdGFP or AdFoxO; (B) Mouse meniscus from AcanCreERT-TKO and control mice, Col2Cre control and Col2Cre-TKO knock-out mice at 6 months old.

SI References

1. Mankin HJ, Dorfman H, Lippiello L, & Zarins A (1971) Biochemical and metabolic abnormalities in articular cartilage from osteo-arthritic human hips. II. Correlation of morphology with biochemical and metabolic data. *J Bone Joint Surg Am* 53(3):523-537.
2. Pritzker KP, *et al.* (2006) Osteoarthritis cartilage histopathology: grading and staging. *Osteoarthritis Cartilage* 14(1):13-29.
3. Outerbridge RE (1961) The etiology of chondromalacia patellae. *J Bone Joint Surg Br* 43-B:752-757.
4. Pauli C, *et al.* (2011) Macroscopic and histopathologic analysis of human knee menisci in aging and osteoarthritis. *Osteoarthritis Cartilage* 19(9):1132-1141.
5. Hyde G, Boot-Handford RP, & Wallis GA (2008) Col2a1 lineage tracing reveals that the meniscus of the knee joint has a complex cellular origin. *J Anat* 213(5):531-538.
6. Nagao M, Cheong CW, & Olsen BR (2016) Col2-Cre and tamoxifen-inducible Col2-CreER target different cell populations in the knee joint. *Osteoarthritis Cartilage* 24(1):188-191.
7. Henry SP, *et al.* (2009) Generation of aggrecan-CreERT2 knockin mice for inducible Cre activity in adult cartilage. *Genesis* 47(12):805-814.
8. Paik JH, *et al.* (2007) FoxOs are lineage-restricted redundant tumor suppressors and regulate endothelial cell homeostasis. *Cell* 128(2):309-323.
9. Glasson SS, Blanchet TJ, & Morris EA (2007) The surgical destabilization of the medial meniscus (DMM) model of osteoarthritis in the 129/SvEv mouse. *Osteoarthritis Cartilage* 15(9):1061-1069.
10. Lu Y, *et al.* (2014) Col10a1-Runx2 transgenic mice with delayed chondrocyte maturation are less susceptible to developing osteoarthritis. *Am J Transl Res* 6(6):736-745.